THE JOURNAL OF PHYSICAL CHEMISTRY A
A JOURNAL OF THE AMERICAN CHEMICAL SOCIETY

pubs.acs.org/JPCA

Article

# Machine Learning and Informatics Based Elucidation of Reaction Pathways for Upcycling Model Polyolefin to Aromatics

*Published as part of The Journal of Physical Chemistry virtual special issue "Early-Career and Emerging Researchers in Physical Chemistry Volume 2".*

Chin-Fei Chang and Srinivas Rangarajan*

Cite This: *J. Phys. Chem. A* 2023, 127, 2958−2966

Read Online

ACCESS | Metrics & More | Article Recommendations | Supporting Information

**ABSTRACT:** Catalytic upcycling of plastics results in a complex network of potentially thousands of reactions and intermediates. Manual analysis of such a network using ab initio methods to identify plausible reaction pathways and rate-controlling steps is intractable. Here, we combine informatics-based reaction network generation and machine learning based thermochemistry calculation to identify plausible (nonelementary step) pathways involved in dehydroaromatization of a model polyolefin, *n*-decane, to form aromatic products. All 78 aromatic molecules found involve a sequence comprising dehydrogenation, $\beta$-scission, and cyclization steps (in slightly different order). The plausible flux-carrying pathway depends on the family of reactions that is rate-controlling while the thermodynamic bottleneck is the first dehydrogenation step of *n*-decane. The adopted workflow is system agnostic and can be applied to understand the overall thermochemistry of other upcycling systems.

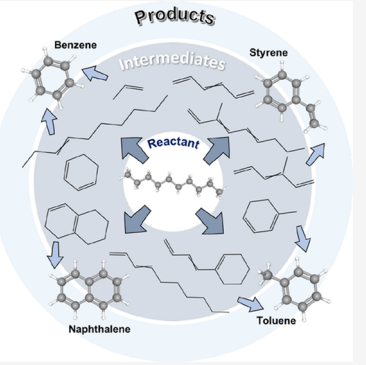


## INTRODUCTION

Upcycling plastics to value-added products presents a promising route to reducing plastic waste. Consequently, while there have been studies on catalytic depolymerization over the last few decades,[1−5] there has been a recent resurgence in research due to increased interest in plastics recycling.[6−10] Multiple approaches have been recently proposed to deconstruct polyolefins, including (1) hydrocracking using a bifunctional metal/zeolite catalyst,[11] (2) hydrogenolysis using molecular hydrogen at high pressure on transition metal catalysts such as Ru,[12,13] (3) processive hydrogenolysis on mesoporous $Pt/SiO_2$ catalyst inspired by macromolecule processive deconstruction by enzymes,[14] (4) tandem dehydrogenation-olefin metathesis using a sacrificial alkane on a mixture of $SnPt/\gamma\text{-}Al_2O_3$ and $Re_2O_7/\gamma\text{-}Al_2O_3$ heterogeneous catalyst system,[15] and (5) tandem chemistry involving bromination, dehydrobromination to produce C−C double bonds, and olefin metathesis with ethylene.[16] All of these approaches involve a coreactant; however, one promising chemistry involves converting polyethylene on a Pt/alumina catalyst, without a coreactant, to produce substituted aromatics (along with byproduct hydrogen).[17] Zhang et al.[17] postulated that the dehydroaromatization of the polymer occurred via a tandem sequence of dehydrogenation, cyclization, and hydrogenolysis on the Pt catalyst, while recent results suggest that acid sites on the support play a role.[18] Understanding the reaction pathways of this system can provide mechanistic insights that can aid in the design of superior catalysts. However, the tandem sequence of steps likely results in thousands of reactions and intermediates, the sheer size of which precludes experimental identification of all relevant intermediates or the flux-carrying pathways. Furthermore, enumerating the upcycling reaction pathways manually and performing ab initio calculations, as is often done for smaller reaction systems, is also intractable; consequently, only a few elementary steps of model polymer molecules have been considered using density functional theory (DFT).[19] While kinetic models of polymer degradation[20] and upcycling[21] have been developed, they often require simplifications such as (1) using averaged kinetics and thermochemistry of reaction steps and (2) approximations such as tracking moments of the polymer chain distribution or invoking a pseudo steady state assumption to reduce the number of differential equations in the model.

As a first step toward a molecular level understanding of the complex networks in polymer upcycling while still keeping the computations tractable, in this work, we develop and employ an automatic workflow to study the reaction pathways and associated thermochemistry of dehydroaromatization of a

**Received:** March 1, 2023
**Revised:** March 13, 2023
**Published:** March 28, 2023

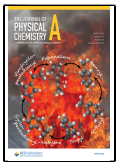







https://doi.org/10.1021/acs.jpca.3c01444
*J. Phys. Chem. A* 2023, 127, 2958−2966

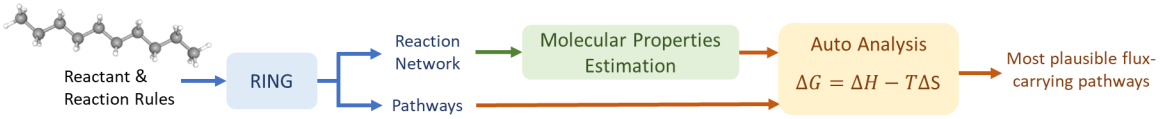


**Figure 1.** An automated network-screening workflow.

model polyolefin molecule. Specifically, we (1) use a cheminformatics-based network generator to construct an upcycling network comprising thousands of (closed shell) intermediates and reactions pertaining to the conversion of a model polyolefin, *n*-decane, to a variety of products using transformations that likely occur on a metal−acid bifunctional catalyst, (2) extract reaction pathways to a variety of alkyl substituted aromatics from decane through graph-based network traversal of the upcycling network, (3) evaluate the gas phase thermochemistry of the individual steps in these pathways using a machine learning based energy calculator, and (4) identify plausible bottlenecks and reaction pathways for *n*-decane conversion. For this analysis, while we ensure that the reactions are generally consistent with the nature of the catalyst, the surface intermediates and the identity of the active site are not explicitly considered. This workflow is, as a result, chemistry agnostic and can be applied to elucidate pathway level information in a variety of other upcycling chemistries.

## COMPUTATIONAL METHODS

The computational workflow developed in this work is illustrated in Figure 1. First, a reaction network is generated using Rule Input Network Generator (or RING)[22,23] with reaction rules corresponding to overall transformations of a bifunctional metal−acid catalytic system. Next, TorchANI,[24] a machine learned energy calculator, is employed to compute the minimum energy structure and the corresponding vibrational frequencies from which standard statistical mechanical treatment within the harmonic approximation affords the computation of standard enthalpies and entropies of all molecules in the network. Finally, an automated screening step extracts likely pathways to aromatic products based on the free energy change of the reaction. In the following sections, each of these steps are discussed in detail.

**Reaction Networks Generation Using RING.** We applied RING to generate an exhaustive network of polymer upcycling reactions. The molecule *n*-decane ($C_{10}H_{22}$) was input as the sole reactant to RING. A set of overall reaction transformations (i.e., nonelementary steps) describing standard metal and acid catalyzed reactions were fed as reaction rules. In particular, the rules are (1) dehydrogenation of a C−C single bond and hydrogenation of a C═C that are likely to occur on metal sites, (2) $\beta$-scission likely to occur on an acid site, (3) isomerization leading to methyl branching, plausibly on an acid site, and (4) cyclization, also occurring on the acid sites of $\gamma$-Alumina.

RING accepts these rules in the form of an English-like language that describes the atoms and bonds participating in the step and the transformations they undergo. Figure 2 depicts the dehydrogenation step; a C−C single bonded moiety containing a C−H bond on each carbon atom undergoes this rule to form a C−C double bond followed by the scission of the two C−H bonds and the formation of an H−H bond. The corresponding rule specification in RING would be as shown in Figure 3. Completed code of all reaction rules are provided in Table S1 (SI Section 1). In addition to

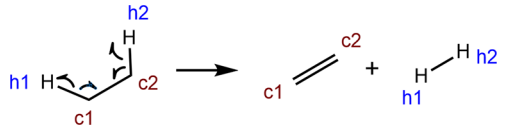


**Figure 2.** Reaction rule of dehydrogenation of a C−C bond.

```
rule dehydrogenation{\newline
reactant r1{
   C labeled c1
   C labeled c2 single bond to c1
   H labeled h1 single bond to c1
   H labeled h2 single bond to c2}
break bond (c1,h1)
break bond (c2,h2)
form bond (h1,h2)
increase bond order (c1,c2)}
```

**Figure 3.** An example rule (dehydrogenation) described using RING's specification language.

these rules, a global constraint, applicable to all molecules generated in the network, was included to restrict the formation of consecutive C−C double bonds (e.g., C═C═C).

Although the chemistry was originally proposed to occur through a tandem hydrogenolysis/aromatization route on the Pt catalyst,[17] a subsequent investigation by Sun et al. investigation byindicates the essential role of the acid sites on the alumina support.[18] Thus, we primarily consider a bifunctional chemistry in this work, although a comparison with the hydrogenolysis pathway is given in the end.

RING generated thousands of species, including various aromatic compounds mimicking those observed experimentally by Zhang et al.[17] Through a graph-traversal based postprocessing query module in RING, we were able to extract these compounds of interest and their synthesis routes, which we analyzed further as discussed below.

**Automatic Analysis in the Reaction Network.** An automated, rapid network-screening workflow using RDKit[25] and TorchANI[24] was developed to analyze the species and reactions in the generated network.

*Computing Thermochemical Properties of the Species in the Network.* Molecules generated in RING, output as 2D SMILES strings, were converted into 3D structures using the experimental-torsion distance geometry[26,27] (ETKDG v2) approach in RDKit which computes an approximate structure using experimental information on bond distances and angles. To identify the minimum energy structure reliably, 200 conformers were generated for each molecule. Each conformer guess was independently relaxed using a geometry optimizer implemented within the atomic simulation environment package (ASE)[28] which interfaced with TorchANI to calculate energy and forces at each iteration. The conformer with the lowest potential energy is thus considered as the globally optimized molecular structure.

The entropy and standard enthalpy were computed based on the statistical mechanical treatment of the ideal gas.



https://doi.org/10.1021/acs.jpca.3c01444
J. Phys. Chem. A 2023, 127, 2958−2966

Specifically, the molecular potential energy and the analytic Hessian matrices used for deriving the vibrational frequencies are all computed through TorchANI. We note that the ANI-1ccx neural network potential[29,30] is applied in this workflow, as it is trained on the CCSD(T)*/CBS data set using transfer learning starting on ANI-1x, a DFT-comparable neural network model with 10× larger data set. The number of atoms per molecule in the data set reaches up to 50 (including H and heavy atoms), thus covering the largest molecule (*n*-decane) in our network. The symmetry information, required for computing the rotational partition function, is acquired from the molecular point group symmetry library, libmsym.[31,32] The calculated entropies across a temperature span is then fitted to a polynomial equation, also known as the Shomate equation. Through the fitted Shomate parameters, we can further estimate the heat capacity at constant pressure ($C_p$) and compute the standard enthalpy ($H$) simply by summing the ground state energy (U), the zero point energy (ZPE) and the integral $\int_{10K}^{298.15K} C_p \, dT$. The computational cost for the molecular properties estimation is about 2.4 min per molecule. Further details of entropy calculation can be obtained from Ochterski's work[33,34] and the accuracy benchmark for TorchANI and the enthalpy estimation of $H_2$ are provided in SI sections 3 and 4.

We note here that the polymer reaction system is in the condensed phase comprising a complex mixture of the unreacted polymer (melt or solid) and an array of intermediates and products. The gas phase thermochemistry, therefore, is not fully representative of the reaction mixture; however, since all molecules in this system are hydrocarbons, we expect that the liquid phase will not influence the relative thermodynamic quantities (e.g., the enthalpy or entropy change of a reaction) significantly. Therefore, we posit that the gas phase thermochemistries are sufficient to screen for plausible reaction pathways, while a more detailed kinetic model that takes into account the corrections due to the solvent is needed to predict rates reliably.

*Pathway Analysis.* RING was used to extract the reaction pathways to target products (e.g., aromatics) using the in-built postprocessing algorithms that traverse the reaction network using a depth-first graph search. Part of the complexity of the upcycling network comes from the multitude of synthesis routes to various products. To understand which pathway is potentially more plausible to achieve, we use thermochemistry as a proxy to screen these pathways.

The Gibbs free energy change ($\Delta G_{rxn}$) of each reaction step in every pathway is first computed from the reaction enthalpy $\Delta H_{rxn}$ and $\Delta S_{rxn} \times T$, where $T$ = 298 K is used. The reaction step with the highest $\Delta G_{rxn}$, i.e., $\Delta G_{max}$ for each pathway, is found. Next, the subset of pathways with the smallest $\Delta G_{max}$ value is selected and referred to as the "min-max" pathways; the step with this free energy value is defined as the bottleneck reaction step. This procedure of finding "min-max" pathways is successively applied on the remaining reaction steps of each of these pathways until one final pathway, which is referred to as the "plausible flux-carrying pathway" is selected.

## RESULTS AND DISCUSSION

**Product Spectrum.** The decane upcycling reaction network contains 24,507 reactions and 3,759 species, underlining the complexity and the rich chemistry of polymer upcycling. The species generated via RING can be classified into three classes: paraffins (1.54%), olefins (42.8%), and cyclics (55.6%). In Figure S2, the three classes are further organized by the carbon number (i.e., the number of carbon atoms) of the molecule. Unsurprisingly, the largest group is the set of molecules with 10 carbon atoms (2,615) since the number of isomers increases exponentially with the number of atoms of the molecule. For molecules containing less than 6 carbons, the ratio of olefin (gray) to paraffinic (orange) molecules increases as the position (and the number) of C−C double bonds in the olefin becomes higher (or larger).

**Statistical Distribution of Reaction Enthalpies.** The upcycling reaction network is composed of thousands of reactions pertaining to the five given rules mentioned in the section of computational methods. Kinetic models of polymerization (and depolymerization) often use single averaged thermochemistry for various reaction steps within a single family. To evaluate this assumption, we investigated the distribution of reaction enthalpy for each of these rules (or families). As shown in Figure 4, dehydrogenation is generally

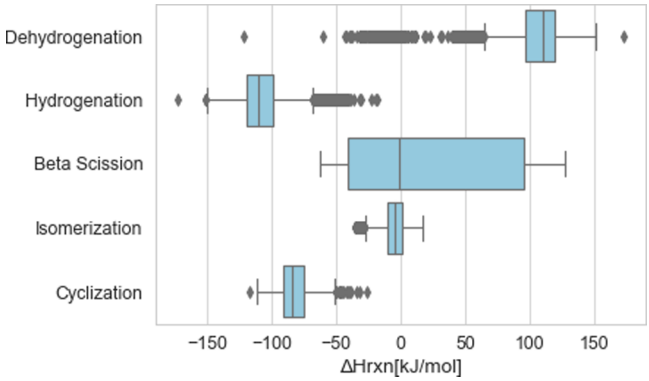


**Figure 4.** A box plot of the distribution of the enthalpy change of reaction for each reaction family.

an endothermic reaction, $\beta$-scission can be exothermic or endothermic, isomerization is slightly exothermic to thermoneutral, and hydrogenation and cyclization are exothermic reactions.

Generally, dehydrogenation and $\beta$-scission to break C−H and C−C bonds, respectively, are endothermic. However, the $\beta$-scission of the ends of an olefinic chain tends to be exothermic; details about the distribution of $\beta$-scission at different positions are provided in Figure S6. Although the interquartile range (97.0−118.9 kJ/mol) of dehydrogenation is far above 0 kJ/mol, we observe that the distribution has a long tail starting from the lower whisker to −121.7 kJ/mol. To understand the origin of this spread, all of the 8,383 dehydrogenation reactions were sorted into three types (Figure S7): dehydrogenation of (A) an acyclic molecule or an alkyl side chain of a cyclic molecule, (B) an endocyclic C−C bond that does not result in an additional aromatic ring, and (C) an endocyclic C−C bond that leads to an additional aromatic ring. The median value of $\Delta H_{rxn}$ of each type of dehydrogenation varies as (A) 114 > (B) 100 > (C) −8 kJ/mol. The first two types (A,B) of dehydrogenation are endothermic since breaking two C−H bonds and forming an unsaturated C═C bond require energy. On the other hand, the dehydrogenation of an endocyclic C−C bond that leads to an increase in the number of aromatic rings (type C) is thermodynamically


https://doi.org/10.1021/acs.jpca.3c01444
J. Phys. Chem. A 2023, 127, 2958−2966

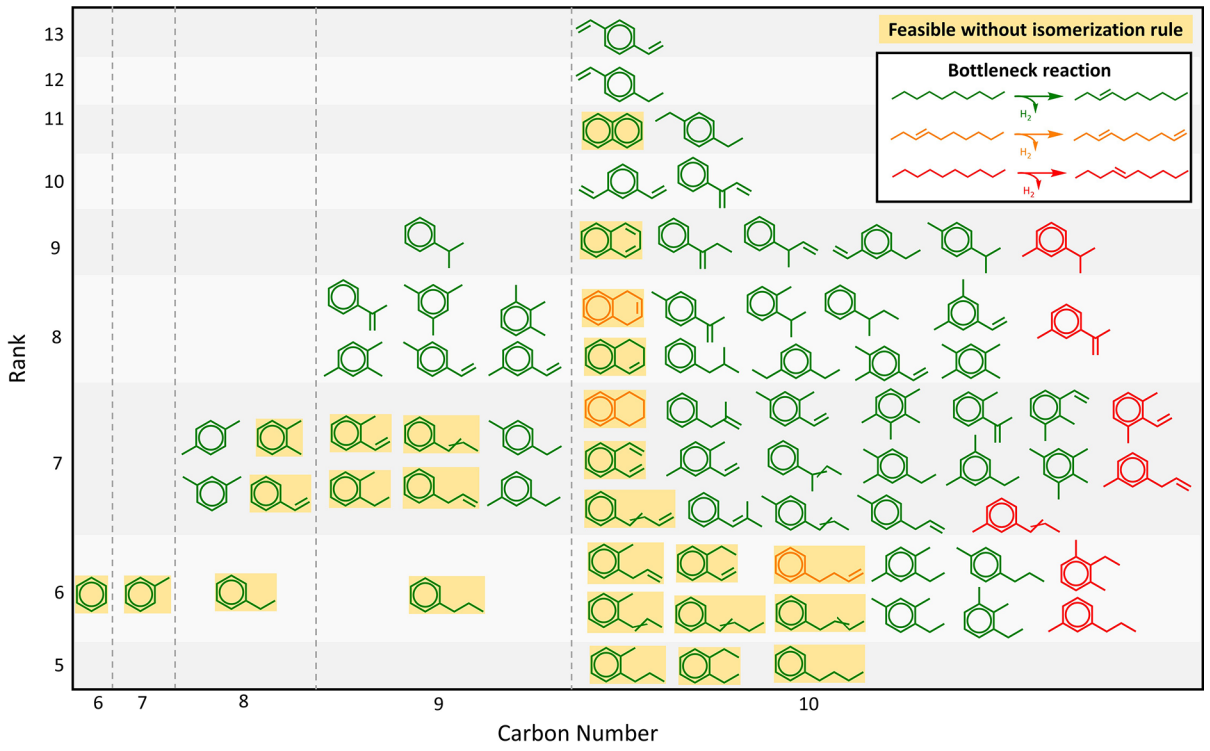


**Figure 5.** Upcycling network found 78 potential aromatic products from *n*-decane. The products are classified with the number of carbons contained in the *x*-axis and the rank (the minimum number of steps required to reach the molecule from the reactant) in the *y*-axis. The 26 molecules in the yellow box can be formed through pathways without isomerization. The bottleneck reactions in the most plausible pathway for each molecule are displayed in the legend and are color-coded.

favorable as the product is resonance stabilized relative to the reactant of that step.

**Potential Aromatics as Upcycling Products.** About 78 of the ∼3700 species in the network are aromatic compounds, the smallest of which is benzene ($C_6H_6$) while the largest aromatics are C10 compounds such as naphthalene and alkyl substituted benzene. All aromatics products are shown in Figure 5 in terms of the carbon number and its rank in the network (i.e., the minimum number of steps required to reach the molecule from the reactant, viz., decane). Table 1 shows the results of pathway queries to different aromatic molecules. In particular, we sought all pathways up to one step longer than the shortest path to each molecule from the initial reactant. There are tens to hundreds of pathways for these aromatic molecules. For instance, RING identified 461 pathways to benzene, of which 42 were of length six (the length of the shortest path to benzene) and 419 of length seven. All of the query results are available in SI section 2.

**Table 1. Results of Pathway Queries to Different Aromatic Molecules**[a]

| Molecule | Number of Pathways | $L_{min}$ | $L_{min+1}$ |
|---|---|---|---|
| Benzene | 461 | 42 | 419 |
| Toluene | 788 | 75 | 713 |
| *p*-Xylene | 591 | 132 | 459 |
| *o*-Xylene | 1,130 | 176 | 954 |
| *m*-Xylene | 1,507 | 207 | 1,300 |
| Ethylbenzene | 165 | 67 | 98 |
| Stryene | 3,471 | 977 | 2,494 |

[a]The number of pathways is a sum of $L_{min}$ and $L_{min+1}$ where $L_{min}$ is the number of pathways of the shortest length and $L_{min+1}$ is the number of pathways of length one more than that of the shortest.

Another way to classify the aromatic products is by the number of alkyl branches (and rings). Specifically, monoalkylbenzenes (21), dialkylbenzenes (33), trialkylbenzenes (15), tetra-alkylbenzenes (3), and polycyclics (5) are the five groups observed in Figure 5 with benzene excluded. It is worth noting that, without the isomerization rule, only 26 aromatic compounds can be formed. All of these 26 aromatics fall into the categories of mono/dialkylbenzenes or polycyclics; i.e., no triple branched or higher branched benzenes are formed. Interestingly, all of the dialkylbenzenes formed in this case are ortho substituted molecules. This is because, in the absence of isomerization, the network mostly has unbranched olefins that are precursors to aromatics. Ring closure of such molecules will lead to either monoalkyl substituents or dialkyl substituents formed by C−C bond formation of the carbon atoms in the second and seventh position (Figure S3). In the latter case, the carbon atoms in the first and eighth positions form the two ortho substituents. On the other hand, when a single-branched or multibranched alkene undergoes ring closure, the branch(es) attached to any carbon(s) between the two reacting carbons are preserved, thereby leading to meta or para substituted cyclics. Since isomerization can occur on acidic sites, the extent and nature of branching of the aromatic products is an indication of the importance of acidic sites.

As discussed so far, in addition to the common aromatic products, i.e., benzene, toluene, and xylenes (BTX), the alkylaromatics and naphthenes reported by Zhang et al.[17] are also found in our reaction network. However, instead of the tandem hydrogenolysis/aromatization via dehydrocyclization proposed in Zhang's work, we report that the similar


https://doi.org/10.1021/acs.jpca.3c01444
J. Phys. Chem. A 2023, 127, 2958−2966

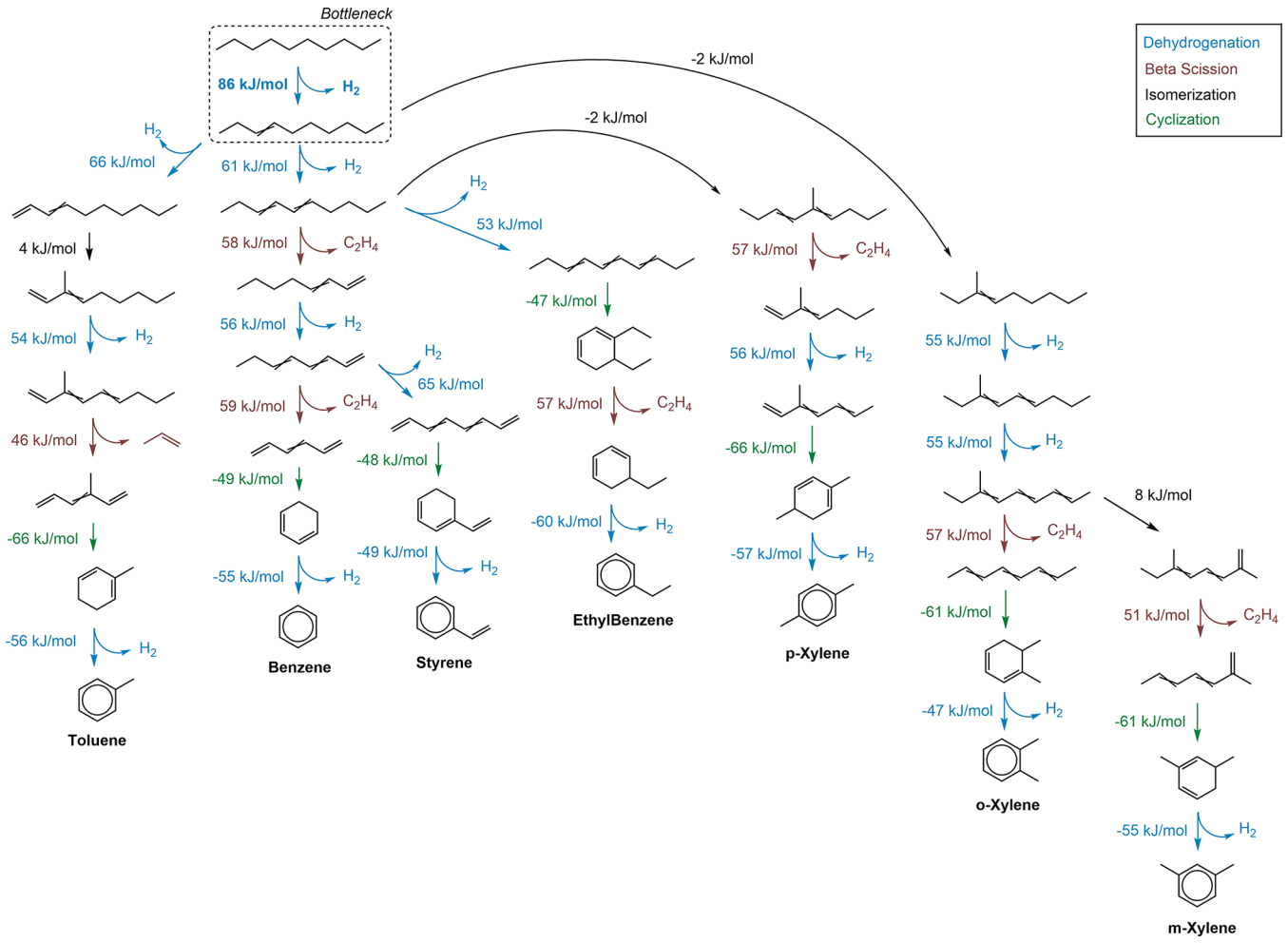


**Figure 6.** Best pathway from *n*-decane to benzene, toluene, xylenes, styrene, and ethylbenzene. All best pathways shared the same bottleneck reaction; different aromatic products can be reached through branched pathway from certain intermediates (3-decene or 3,5-decadiene, for example).

alkylaromatics and naphthenes can be converted through pathways composed of dehydrogenation, cyclization, $\beta$-scission, and isomerization, which is consistent with a subsequent presentation from the same team.[18] The molecule 1-methyl-2-propylbenzene, a 10-carbon dialkylbenzene with a rank of five, can be obtained from a five-step pathway comprising four dehydrogenation steps with one cyclization step after the second dehydrogenation. This molecule can also be obtained via six-step pathways with one additional isomerization step that converts the unbranched alkene to a branched alkene, which always occurs before the cyclization step. In cases where the aromatics contain fewer than 10 carbons, e.g., 1-ethyl-2-methylbenzene, the pathway will include at least one $\beta$-scission that breaks the long carbon chain into smaller ones.

As partly revealed in Table 1, the number of reaction pathways from decane upcycling to various products can be large. Figure S4 shows that the number of total pathways of an aromatic product increases exponentially with the rank of the molecule. The molecule 1,4-divinylbenzene, with rank 13, has the highest number of total pathways (~52,000). Many other molecules have more than 10,000 reaction pathways; the average number of pathways for the 78 aromatic products is around 2,700. Evidently, the number of the pathways is large enough that it is necessary to screen for the most likely pathways in an automated fashion. To this end, we use the "min-max" selection procedure described earlier.

The "min-max" pathways from decane to each of the aromatic molecules and the corresponding bottleneck reaction step were identified (per Computational Methods) and results are available in SI section 5. Briefly, the bottleneck reaction of each aromatic upcycling pathway has $\Delta G_{rxn}$ ranging from 86.3 to 88.1 kJ/mol and is either the first or the second dehydrogenation step in the pathway. The dehydrogenation of decane to 3-decene is the thermodynamic bottleneck step for 68 aromatic compounds and has a relatively low $\Delta G_{rxn}$ compared to 3-decene dehydrogenated to 1,7-decadiene (which is the thermodynamic bottleneck for 3 aromatic compounds) and decane to 4-decene (which is the thermodynamic bottleneck for 7 aromatic compounds). It is not surprising that dehydrogenation requires a higher Gibbs energy change compared to the other four reaction rules, given the distribution reported in Figure 4.

**Most Plausible Flux-Carrying Pathways from *n*-Decane to Common Aromatics.** Having identified the bottleneck reaction steps, the pathways sharing the same bottleneck were further investigated by iteratively applying the min-max criterion (as explained earlier) in order to find the most plausible flux-carrying pathway for each aromatic compound. For instance, benzene has 461 pathways. Its first


https://doi.org/10.1021/acs.jpca.3c01444
J. Phys. Chem. A 2023, 127, 2958−2966

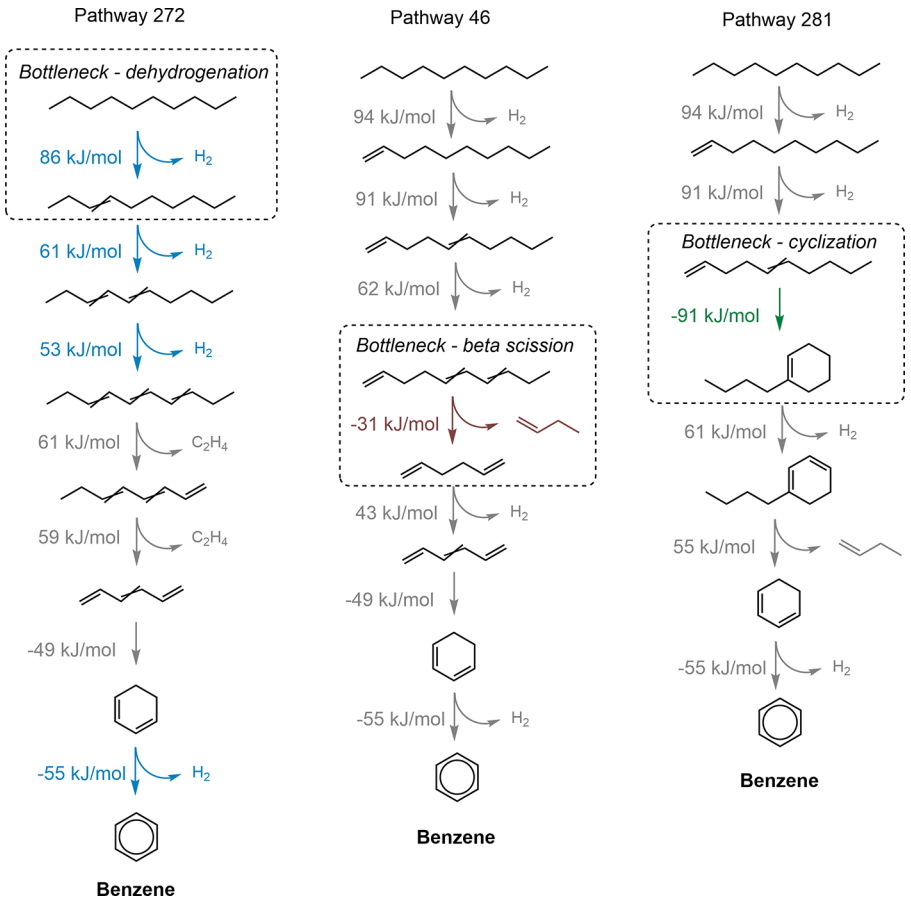


**Figure 7.** Plausible flux-carrying pathways for benzene from *n*-decane assuming different rules are rate-controlling. In this case, multiple pathways can be found as the most plausible one since the subset of the dehydrogenation step(s) or $\beta$-scission step(s) or cyclization step(s) of pathways may be identical; only one representative pathway is shown for each rule.

"min-max" bottleneck reaction is the first dehydrogenation (decane to 3-decene) and is shared by 55 of the 461 pathways. Starting with these 55 pathways, we followed the process of finding the "min-max" steps repeatedly on the remaining portion of the pathways (i.e., the second step and further) so as to systematically prune down the 55 plausible pathways and find the most plausible pathway (or the "best" pathway). The pruning process takes a few seconds to a minute depending on the number of all potential pathways. The best pathway to benzene is illustrated in the left part of Figure 6.

Thermodynamically speaking, decane favors the pathway undergoing the following sequence: (i) two dehydrogenation steps, (ii) one $\beta$-scission step resulting in a ethylene molecule, (iii) a third dehydrogenation step, (iv) a second $\beta$-scission step resulting in one ethylene molecule, and (v) one cyclization step followed by (vi) a dehydrogenation to convert into one benzene. This is a seven-step pathway, which is one step longer than the shortest pathway to benzene (which is of rank six; see Figure 5). Thus, from a thermodynamic standpoint, the shortest upcycling pathway is not necessarily the most favored one.

The process of identifying the "min-max" pathways was carried out on toluene, xylenes, styrene, and ethylbenzene as these are common raw materials applied in manufacturing high-value chemical products. The corresponding plausible flux-carrying pathways (on the basis of thermodynamics) for each of the these aromatics is shown in Figure 6. The most plausible flux-carrying pathway for these seven molecules shown in Figure 6 shares the same bottleneck, viz., the dehydrogenation of decane to 3-decene. The 3-decene can be further dehydrogenated into 1,3-decadiene, which leads to toluene eventually; it can also be dehydrogenated into 3,5-decadiene and ultimately lead to benzene, styrene, ethylbenzene, or *p*-xylene. In the case where 3-decene isomerizes to 3-methylnonene, it may upcycle to *o*-xylene or *m*-xylene if another isomerization occurs on the 7-methylnona-2,4,6-triene. The pathways and products map reveals part of the complexity of the reaction network under study. Several intermediates, such as 3-decene or 3,5-decadiene, act as branch points and judicious selection of catalysts could allow for tuning the product selectivity.

While kinetic information is a more appropriate metric to screen plausible pathways, computing kinetic parameters, particularly of elementary catalytic steps, using ab initio methods would be computationally prohibitive. A scalable alternative would be to develop data-driven energy potentials; however, off-the-shelf models for hydrocarbons encountered here (and surface intermediates derived from them) on metal or acid catalysts (e.g., platinum or alumina) do not currently exist and will have to be trained. Instead, as a first approximation, we posit that gas phase thermodynamics of the nonelementary steps can be employed to identify bottleneck reactions as well as flux-carrying pathways. This is because rules such as dehydrogenation, beta scission, and oligomerization follow linear free energy relationships; therefore, a more endothermic step has a higher activation barrier


https://doi.org/10.1021/acs.jpca.3c01444
J. Phys. Chem. A 2023, 127, 2958−2966

than a relatively exothermic step of the same rule.[35−37] However, these relationships are typically catalyst dependent and are not available for the catalysts assumed in this work; therefore, the barriers of reactions of two different rules cannot be compared either quantitatively or qualitatively. Instead, we examined plausible pathways assuming that rate-controlling steps can only belong to one family of reactions (e.g., only dehydrogenation or beta scission); this simplification allows us to qualitatively compare two reactions of the same rule based on their reaction energetics (more endothermic or endergonic a step is, the higher is its activation barrier).

We slightly modified our procedure of finding plausible "min-max" pathways by only considering reactions of one specific rule at a time. In this case, multiple pathways can be identified to be equally plausible because they essentially have the same set of reactions of the rate-controlling rule (while other steps may be different).

For benzene, the first step is the kinetic bottleneck, if the dehydrogenation steps are rate-controlling (i.e., only dehydrogenation steps are screened in the "min-max" pathways). However, different pathways would be deemed plausible if other rules are controlling. Figure 7 shows the plausible pathways if a step corresponding to dehydrogenation, $\beta$-scission, or cyclization is rate-controlling. Analysis of plausible pathways on the other six aromatic products shown in Figure 6 with $\beta$-scission as the rate-controlling step can be seen in Figure S5. While this analysis does not identify the kinetically significant route, it does allow for pruning the network to consider only a small subset of pathways (e.g., only those shown in Figure 7 for benzene).

**Reaction Network with Hydrogenolysis.** We finally consider a reaction network using reaction rules considered by Zhang et al.[17] To this end, we replaced the $\beta$-scission rule with hydrogenolysis rule (whereby a C−C bond is broken to form 2 C−H bonds using molecular hydrogen as a coreactant) and a cyclization rule that essentially is an intramolecular C−C bond formation rule. We regenerated a reaction network consisting of four reaction rules only (hydrogenation, dehydrogenation, hydrogenolysis, and cyclization; details in SI section 1). The statistical distribution of reaction enthalpies (Figure S10) shows that hydrogenolysis is an exothermic reaction and the modified cyclization rule is slightly endothermic.

Only 21 aromatics (see Figure S8) were found in the network, and these are a subset of the previously found 78 aromatics in Figure 5. The alkylaromatics in this list are all in the ortho position and the rank is smaller by one (i.e., it takes fewer steps to form these molecules). Similarly, the bottleneck reaction step was identified through our *min-max* procedure (SI section 5) and it was found that generally the dehydrogenation on the C−C single bond of a cyclohexane is the bottleneck reaction step, except for 1-allyl-2-methylbenzene which has the dehydrogenation on the end acyclic C−C single bond as the bottleneck reaction step.

The plausible flux-carrying pathways from *n*-decane to common aromatics are shown in Figure S9. A cyclization step is required to create a C6 ring, and the hydrogen molecule generated here is consumed in the hydrogenolysis steps. Different branches from one common intermediate can form different aromatics (for instance, 1-propylcyclohexene can lead to toluene, styrene, or ethylbenzene).

We re-emphasize that our method does not include surface intermediates and their energies. A different catalyst will lead to a difference in energetics of surface intermediates (not considered here), thereby leading to different reaction rates; nevertheless, qualitative pathway-level information will remain the same as these depend only on bulk thermochemistry. That is, our qualitative insights of thermodynamic bottlenecks and potential rate-controlling steps will hold across different catalysts with similar overall transformation rules.

## CONCLUSIONS

In this work, we studied the plausible reaction pathways of dehydroaromatization of a model polyolefin, *n*-decane, to aromatics using a novel workflow. First, all plausible reaction pathways of *n*-decane conversion on a metal−acid bifunctional catalyst were generated using RING, a cheminformatics-based network generation software. Among the 24,000 reactions and 3,759 species that were generated, we found 78 alkylaromatic products, many of which are also experimentally seen. Without isomerization on unbranched alkene, however, only 26 aromatics in the groups of alkylbenzene, dialkylbenzene, or naphthalene can be formed, indicating the importance of this chemistry that results in product diversity. The reaction pathways to common aromatic products were assessed based on gas phase thermochemistry using a machine learned potential in order to identify bottleneck steps and the most likely upcycling pathway for each product quickly (2.4 min per molecular property and up to 1 min per product pathway). The thermodynamically challenging reaction turns out to be the first or the second dehydrogenation step as the reaction rule of dehydrogenation has the highest $\Delta H_{rxn}$ compared to others. The most thermodynamically favored pathways to benzene, toluene, xylenes, styrene, and ethylbenzene were analyzed in detail, and the results show common intermediates that serve as branch points to form each of the products (and potentially others). Since these may not be kinetically controlling, the idea of linear free energy relationships that often govern reaction families were invoked to identify plausible kinetic bottlenecks using thermochemistry alone. For each reaction family, we identified the pathway which would be flux-carrying if that family were rate-controlling. While this workflow (1) neglects the catalyst and surface intermediates, (2) does not include kinetics information explicitly, and (3) employs gas phase thermochemistry, we posit that the results still enable us to identify plausible overall reaction steps and specifically explain the formation of aromatics as involving a series of dehydrogenation, beta scission, and cyclization (followed by dehydrogenation) steps. The pathways identified here can be further examined using ab initio methods to compute the kinetic barriers of elementary steps (and build kinetic models). This method is system agnostic and can be applied to study any other polymer upcycling reactions.

## ASSOCIATED CONTENT

### Supporting Information

The Supporting Information is available free of charge at https://pubs.acs.org/doi/10.1021/acs.jpca.3c01444.

Additional details on computational methods and figures for the Results and Discussion, including links to all applied scripts (RING and python files) and analysis results (PDF)



https://doi.org/10.1021/acs.jpca.3c01444
J. Phys. Chem. A 2023, 127, 2958−2966

## AUTHOR INFORMATION


### Corresponding Author

**Srinivas Rangarajan** − *Department of Chemical & Biomolecular Engineering, Lehigh University, Bethlehem, Pennsylvania 18015, United States;* orcid.org/0000-0002-6777-9421; Email: srr516@lehigh.edu

### Author

**Chin-Fei Chang** − *Department of Chemical & Biomolecular Engineering, Lehigh University, Bethlehem, Pennsylvania 18015, United States*

Complete contact information is available at: https://pubs.acs.org/10.1021/acs.jpca.3c01444


### Notes

The authors declare no competing financial interest.

## ACKNOWLEDGMENTS

The authors acknowledge partial financial support from the National Science Foundation (NSF), Award numbers 1953245 and 2045550. Parts of this research were carried out on the supercomputing cluster Hawk at Lehigh University which was supported through an award from the NSF (2019035).

## REFERENCES


(1) Onu, P.; Vasile, C.; Ciocılteu, S.; Iojoiu, E.; Darie, H. Thermal and Catalytic Decomposition of Polyethylene and Polypropylene. *J. Anal. Appl. Pyrolysis* **1999**, *49*, 145−153.

(2) Mosio-Mosiewski, J.; Warzala, M.; Morawski, I.; Dobrzanski, T. High-Pressure Catalytic and Thermal Cracking of Polyethylene. *Fuel Process. Technol.* **2007**, *88*, 359−364.

(3) Uemichi, Y.; Nakamura, J.; Itoh, T.; Sugioka, M.; Garforth, A. A.; Dwyer, J. Conversion of Polyethylene into Gasoline-Range Fuels by Two-Stage Catalytic Degradation Using Silica-Alumina and HZSM-5 Zeolite. *Ind. Eng. Chem. Res.* **1999**, *38*, 385−390.

(4) Serrano, D. P.; Aguado, J.; Escola, J. M. Catalytic Cracking of a Polyolefin Mixture over Different Acid Solid Catalysts. *Ind. Eng. Chem. Res.* **2000**, *39*, 1177−1184.

(5) Serrano, D. P.; Aguado, J.; Escola, J. M. Developing Advanced Catalysts for the Conversion of Polyolefinic Waste Plastics into Fuels and Chemicals. *ACS Catal.* **2012**, *2*, 1924−1941.

(6) Korley, L. T. J.; Epps, T. H.; Helms, B. A.; Ryan, A. J. Toward Polymer Upcycling-Adding Value and Tackling Circularity. *Science* **2021**, *373*, 66−69.

(7) Weckhuysen, B. M. Creating Value From Plastic Waste. *Science* **2020**, *370*, 400−401.

(8) Britt, P. F.; Coates, G. W.; Winey, K. I.; Byers, J.; Chen, E.; Coughlin, B.; Ellison, C.; Garcia, J.; Goldman, A.; Guzman, J.; et al. *Report of the Basic Energy Sciences Roundtable on Chemical Upcycling of Polymers*; OSTI, 2019 (accessed Jan 25, 2022).

(9) Chen, X.; Wang, Y.; Zhang, L. Recent Progress in the Chemical Upcycling of Plastic Wastes. *ChemSusChem* **2021**, *14*, 4137−4151.

(10) Mark, L. O.; Cendejas, M. C.; Hermans, I. The Use of Heterogeneous Catalysis in the Chemical Valorization of Plastic Waste. *ChemSusChem* **2020**, *13*, 5808−5836.

(11) Liu, S.; Kots, P. A.; Vance, B. C.; Danielson, A.; Vlachos, D. G. Plastic Waste to Fuels by Hydrocracking at Mild Conditions. *Sci. Adv.* **2021**, *7*, No. eabf8283.

(12) Rorrer, J. E.; Beckham, G. T.; Román-Leshkov, Y. Conversion of Polyolefin Waste to Liquid Alkanes with Ru-Based Catalysts under Mild Conditions. *JACS Au* **2021**, *1*, 8−12.

(13) Wang, C.; Xie, T.; Kots, P. A.; Vance, B. C.; Yu, K.; Kumar, P.; Fu, J.; Liu, S.; Tsilomelekis, G.; Stach, E. A.; et al. Polyethylene Hydrogenolysis at Mild Conditions over Ruthenium on Tungstated Zirconia. *JACS Au* **2021**, *1*, 1422−1434.

(14) Tennakoon, A.; Wu, X.; Paterson, A. L.; Patnaik, S.; Pei, Y.; LaPointe, A. M.; Ammal, S. C.; Hackler, R. A.; Heyden, A.; Slowing, I. I.; et al. Catalytic Upcycling of High-Density Polyethylene via a Processive Mechanism. *Nat. Catal.* **2020**, *3*, 893−901.

(15) Ellis, L. D.; Orski, S. V.; Kenlaw, G. A.; Norman, A. G.; Beers, K. L.; Román-Leshkov, Y.; Beckham, G. T. Tandem Heterogeneous Catalysis for Polyethylene Depolymerization via an Olefin-Intermediate Process. *ACS Sustainable Chem. Eng.* **2021**, *9*, 623−628.

(16) Zeng, M.; Lee, Y.-H.; Strong, G.; LaPointe, A. M.; Kocen, A. L.; Qu, Z.; Coates, G. W.; Scott, S. L.; Abu-Omar, M. M. Chemical Upcycling of Polyethylene to Value-Added $\alpha,\omega$-Divinyl-Functionalized Oligomers. *ACS Sustainable Chem. Eng.* **2021**, *9*, 13926−13936.

(17) Zhang, F.; Zeng, M.; Yappert, R. D.; Sun, J.; Lee, Y.-H.; LaPointe, A. M.; Peters, B.; Abu-Omar, M. M.; Scott, S. L. Polyethylene Upcycling to Long-Chain Alkylaromatics by Tandem Hydrogenolysis/Aromatization. *Science* **2020**, *370*, 437−441.

(18) Sun, J.; Lee, Y.-H.; Abu-Omar, M. M.; Scott, S. L. The Essential Effect of Support Acidity on the Tandem Conversion of Polyethylene to Alkylaromatics. *Proceedings of the 27th North American Catalysis Society Meeting*; North American Catalysis Society, 2022 (accessed June 12, 2022).

(19) Celik, G.; Kennedy, R. M.; Hackler, R. A.; Ferrandon, M.; Tennakoon, A.; Patnaik, S.; LaPointe, A. M.; Ammal, S. C.; Heyden, A.; Perras, F. A.; et al. Upcycling Single-Use Polyethylene into High-Quality Liquid Products. *ACS Cent. Sci.* **2019**, *5*, 1795−1803.

(20) Kruse, T. M.; Woo, O. S.; Wong, H.-W.; Khan, S. S.; Broadbelt, L. J. Mechanistic Modeling of Polymer Degradation: [[TnqNmdEntities]]thinsp;[[/TnqNmdEntities]] A Comprehensive Study of Polystyrene. *Macromolecules* **2002**, *35*, 7830−7844.

(21) Guironnet, D.; Peters, B. Tandem Catalysts for Polyethylene Upcycling: A Simple Kinetic Model. *J. Phys. Chem. A* **2020**, *124*, 3935−3942.

(22) Rangarajan, S.; Bhan, A.; Daoutidis, P. Language-Oriented Rule-Based Reaction Network Generation and Analysis: Description of RING. *Comput. Chem. Eng.* **2012**, *45*, 114−123.

(23) Rangarajan, S.; Kaminski, T.; Van Wyk, E.; Bhan, A.; Daoutidis, P. Language-Oriented Rule-Based Reaction Network Generation and Analysis: Algorithms of RING. *Comput. Chem. Eng.* **2014**, *64*, 124−137.

(24) Gao, X.; Ramezanghorbani, F.; Isayev, O.; Smith, J. S.; Roitberg, A. E. TorchANI: A Free and Open Source PyTorch-Based Deep Learning Implementation of the ANI Neural Network Potentials. *J. Chem. Inf. Model.* **2020**, *60*, 3408−3415.

(25) Landrum, G.; Tosco, P.; Kelley, B.; Ric; Sriniker; Gedeck; Vianello, R.; Schneider, N.; Kawashima, E.; Dalke, A.; et al. *Rdkit/Rdkit: 2021_09_4 (Q3 2021) Release*; Zenodo, 2022; DOI: 10.5281/zenodo.5835217 (accessed Jan 27, 2022).

(26) Riniker, S.; Landrum, G. A. Better Informed Distance Geometry: Using What We Know to Improve Conformation Generation. *J. Chem. Inf. Model.* **2015**, *55*, 2562−2574.

(27) Guba, W.; Meyder, A.; Rarey, M.; Hert, J. Torsion Library Reloaded:A New Version of Expert-Derived SMARTS Rules for Assessing Conformations of Small Molecules. *J. Chem. Inf. Model.* **2016**, *56*, 1−5.

(28) Larsen, A. H.; Mortensen, J. J.; Blomqvist, J.; Castelli, I. E.; Christensen, R.; Dułak, M.; Friis, J.; Groves, M. N.; Hammer, B.; Hargus, C.; et al. The Atomic Simulation Environment—A Python Library for Working with Atoms. *J. Phys.: Condens. Matter* **2017**, *29*, 273002.

(29) Smith, J. S.; Nebgen, B. T.; Zubatyuk, R.; Lubbers, N.; Devereux, C.; Barros, K.; Tretiak, S.; Isayev, O.; Roitberg, A. E. Approaching Coupled Cluster Accuracy with a General-Purpose Neural Network Potential Through Transfer Learning. *Nat. Commun.* **2019**, *10*, 2903.

(30) Smith, J. S.; Zubatyuk, R.; Nebgen, B.; Lubbers, N.; Barros, K.; Roitberg, A. E.; Isayev, O.; Tretiak, S. The ANI-1ccx and ANI-1x Data Sets, Coupled-Cluster and Density Functional Theory Properties for Molecules. *Sci. Data* **2020**, *7*, 134.

(31) Johansson, M.; Veryazov, V. Automatic Procedure for Generating Symmetry Adapted Wavefunctions. *J. Cheminf.* **2017**, *9*, 8.
(32) Johansson, M. *Libmsym*, v0.2.2: Molecular Point Group Symmetry Library, 2015; https://github.com/mcodev31/libmsym, (accessed June 12, 2022).
(33) Ochterski, J. W. *Thermochemistry in Gaussian*. 2000; https://gaussian.com/thermo/ (accessed Aug 25, 2022).
(34) Ochterski, J. W. *Vibrational Analysis in Gaussian*. 1999; https://gaussian.com/vib/ (accessed Aug 25, 2022).
(35) Dill, K. A.; Bromberg, S. *Molecular Driving Forces: Statistical Thermodynamics in Biology, Chemistry, Physics, and Nanoscience*, 2nd ed.; Garland Science: London, 2011; Chapter 19.
(36) Bligaard, T.; Nørskov, J.; Dahl, S.; Matthiesen, J.; Christensen, C.; Sehested, J. The Brønsted−Evans−Polanyi Relation and the Volcano Curve in Heterogeneous Catalysis. *J. Catal.* **2004**, *224*, 206−217.
(37) Wang, S.; Temel, B.; Shen, J.; Jones, G.; Grabow, L. C.; Studt, F.; Bligaard, T.; Abild-Pedersen, F.; Christensen, C. H.; Nørskov, J. K. Universal Brønsted-Rvans-Polanyi Relations for C−C, C−O, C−N, N−O, N−N, and O−O Dissociation Reactions. *Catal. Lett.* **2011**, *141*, 370−373.



https://doi.org/10.1021/acs.jpca.3c01444
*J. Phys. Chem. A* 2023, 127, 2958−2966